International Journal of Chemical Science
Online ISSN: 2523-2843, Print ISSN: 2523-6075; Impact Factor: RJIF 5.22
Received: 01-11-2019; Accepted: 02-12-2019; Published: 09-01-2020
www.chemicaljournals.com
Volume 4; Issue 1; 2020; Page No. 01-08

Kinetic and thermodynamic studies on adsorption of lead (ii) ions from aqueous solutions using polymer-modified coconut shell activated carbon (MCSAC)

Onyedikachi G Okpara[1*], Osareme M Ogbeide[2], Emmanuel C Ezeh[3], Jude I Chukwuekeh[4], Okike D Nwankwo[5], Christopher N Igwilo[6]

[1, 2, 4-6] Department of Science Laboratory Technology, Federal College of Agriculture, P.M.B, Ishiagu, Ebonyi State, Nigeria
[2] Department of Industrial Chemistry, Enugu State University of Science and Technology, P.M.B, Agbani, Enugu, Nigeria

Abstract

Adsorption of lead (II) ions from aqueous solutions on low cost adsorbent prepared from coconut shell modified with polysiloxane was studied experimentally. The adsorption kinetics and thermodynamics were also investigated in batch experiments considering the time and temperature range of 5-20 minutes and 20-80 °C respectively. The removal efficiency (99.9%) of lead (II) ions was obtained at pH 8.0 and 20 minutes contact time. Pseudo-first order, pseudo-second order, Elovich and Intraparticle diffusion were employed to describe the rate of adsorption process, and the potential rate-controlling step on the adsorbent surface. This indicated that the pseudo-second order fits the data better. Thermodynamic parameters such as Gibb's free energy (ΔG^{o}), Enthalpy (ΔH^{o}), Entropy (ΔS^{o}) and Activation energy (Ea) for the adsorption process were evaluated as -22.462 kJmol^{-1}, -25.142 kJmol^{-1}, -8.131 kJmol^{-1}K^{-1} and -57.341 kJmol^{-1} respectively. These values show that the adsorption of lead (II) ions on MCSAC was exothermic and spontaneous in nature.

Keywords: adsorption kinetics, thermodynamics, lead (ii) ions, activated carbon from coconut shell, modification with polymer

1. Introduction

Heavy metals are released into the environment by both natural and anthropogenic activities such as mining, milling, quarrying, smelting operations, other industrial activities, domestic and agricultural use of metals and metal compounds. Other sources of heavy metal contamination into the environment are through metal corrosion, atmospheric deposition, soil erosion of metal ions and leaching [1]. Their occurrence and depositions in high concentration from various manufacturing processes has created a serious environmental issue that are detrimental to the ecosystems through bioaccumulation in organisms, plants, animals, and food chain, causing toxic effects on living organisms and man.

One of the heavy metals considered toxic to humans, animals, fishes and environment is lead. In light of the report by [2], the major sources of lead released into the environment are from metal finishing industries, paint manufacture, electroplating, metallurgical industry, petroleum refining, fuel combustion, photographic materials, lead-acid battery manufacture and drainage from ore and mines. Drinking water delivered through lead pipes or pipes joined with lead solder may contain lead [3]. However, the disposal of lead wastewater without proper treatment is a big challenge and has caused harm to the aquatic environment, such as cancer, accumulative poisoning, nervous system damage, lowering of the reproductive activities of organisms, inhibition of growth, cardiovascular and neurological diseases as well as death in most living beings [4]. Therefore, it must be removed from municipal and industrial effluents channeled into the environment using the conventional methods such as; chemical precipitation, filtration, ion exchange, reverse osmosis, sedimentation, solvent extraction, ultra-filtration, electrochemical deposition, coagulation and adsorption [5, 6]. Due to low biodegradability of the metal wastes, the conventional biological wastewater treatment methods stated above may not always be economically suitable because of their been expensive, time consuming, differ in efficiency, and can generate toxic sludge while some requires higher energy in treating. It is therefore necessary to search for low cost alternative techniques that may be effective, superior, economical, simple to design, ease of operation, sludge free, and non-toxicity of the utilized adsorbents [7]. Thus, adsorption technique, which is based on the transfer of pollutants from the solution to the solid phase, is a great demand [8, 9, 2].

Activated carbon, a widely used adsorbent in industrial Processes is preferred and more viable option for removal of lead from wastewater. it is composed of a microporous, homogenous structure with high surface area and shows radiation stability [10]. In the course of exploring effective and low-cost activated carbon, many adsorbent from agricultural by-products have been applied for the removal of lead (II) ions such as activated carbon from the precursors; palm karnel shell [11], Date pit [12], thevetia neriifolia nutshell [13], rice husk [14], Nano-silver coated activated carbon [15], Cedar leaf [16], plaintain peels [17], eggshells [18], coconut husk [19], coconut shell [20, 21].

Coconut shell activated carbon (CSAC) is an attractive and economic alternative adsorbent utilized in this study, it was modified with immobilized polysiloxanes, to increase the functional group and improve selective properties of coconut shell to adsorb the heavy metal, Pb (II) ions through the formation of coordination compound between them [6, 22]. Hence, the applicability of this modified coconutshell

Activated carbon (MCSAC) in removal of lead (II) ions from aqueous solution was investigated. The effect of temperature, time as well as fitting of adsorption data into various kinetic and thermodynamic equations was studied.

2. Material and Methods

2.1 Materials and Instruments

All the reagents used in this work was of analytical grade; lead nitrate, Pb $(NO_3)_2$ (99 % Labosi, India), 0.1N NaOH, and 0.1N HCl. The instruments used was Flame Atomic Absorption Spectrophotometer FS240AA Agilent U.S.A., Buck scientific M530 USA FTIR was used for the analysis, and SEM-Phenom ProX by Phenom World Eindhoven, Netherlands.

2.2 Methods

2.2.1 Preparation of Coconut shell activated carbon (CSAC)

Coconut shells were thoroughly washed with sponge and clean water severally to remove dirt and subsequently oven-dried at 105 °C for 5hr. The dried shells was crushed into smaller pieces for easy activation. And was loaded into a heat chamber of electric heat muffle furnace to pyrolyse in the absence of air, at temperature raised to 650 °C for 1.30 min, then the furnace was switch off. The substance was kept to cool overnight, after that, the activated carbon was collected, grounded and sieved to fine particles, then stored in air tight container for further use [2].

2.2.2 Preparation of urea immobilized polysiloxane

Tetraethoxysilane (20.83g) was mixed with 15 cm^3 of methanol and 9.95 cm^3 of HCl (0.42 g/cm^3) and stirred very well. 3-chloropropyltriethoxsilane was then added to the mixture and stirred. Gelation occurred after few seconds, and the product was allowed to stand for 12 h, at ambient temperature (room temperature) and then dried in an oven at 90°C. The dried product was grounded, sieved, and washed successively with 50 cm^3 portions of 0.025 g/cm^3 NaOH, water, methanol and diethylether. It was dried again in an oven at 90°C for 10 h. The product (1.0g) was refluxed with 0.98 g of urea in 50 cm^3 of toluene at 110°C for 10 h. After which, it was allowed to cool, filtered, and washed with equal portion of 50 cm^3 water, methanol, and diethyl ether, and dried at 90°C and 1 atm. for 10 h [23].

2.2.3 Modification of activated carbon (CSAC) with urea immobilized polysiloxane

The method described by [2] was employed; 0.5g of the prepared urea immobilized polysiloxane was added to small quantity of de-ionized water. 20g of the activated carbon was added and mixed properly. The mixture was dried in an oven at 50 °C at 150 rpm for about 45 min. After which, the modified coconut shell activated carbon (MCSAC) was formed and ready to be used for the adsorption experiments.

2.3 Characterization of Modified coconut shell activated carbon (MCSAC).

In order to detect the functional groups present in MCSAC. The Fourier Transform Infrared Spectrometer (FTIR) were analysed in spectral range of 4000–600 cm-1. The surface morphology of the MCSAC was analyzed by scanning electron microscopy (SEM) at an accelerating voltage of 15 kV. Also, with EDX analysis to study the elemental composition of the MCSAC.

2.4 Preparation of 1000 ppm Pb $(NO_3)_2$ stock solution

Stock solution was prepared using analytical grade lead nitrate, Pb $(NO_3)_2$ (99 % Labosi, India). To prepare 1000 ppm of $Pb(NO_3)_2$, 1.599g of $Pb(NO_3)_2$ was weighed and then dissolved in 100 cm^3 of distilled water and made up to the mark of 1000cm^3 standard volumetric flask. 0.1 N HCl and 0.1 N NaOH were used for pH value adjustment.

2.5 Batch adsorption experiments

Batch experiments were carried out to study the kinetics and thermodynamic ability of adsorb Pb (II) ion onto modified coconut shell activated carbon (MCSAC). For kinetic studies, 10 ml of 200 mg/l of Pb (II) solutions with pH value 8.0 was transferred to a conical flask containing 0.2 g of MCSAC adsorbent. The solution was shaken at 100 rpm in a Gemmy orbit shaker (model: VRN-480, USA) for different interval time (5, 10, 15 and 20 min) at temperatures 20 °C and 40 °C. And thermodynamic studies was carried out using the same volume of 200 mg/l of Pb (II) solution and same amount of adsorbent at different temperatures of 20 °C, 40 °C, 60 °C and 80 °C for 15 minutes to establish equilibrium condition. After filtration, the aliquots of the supernatant solutions were withdrawn and analyzed using an atomic absorption spectrophotometer (FS240AA Agilent U.S.A).

The amount of lead ion adsorbed per unit mass of the adsorbent (amount adsorbed in mg/g), q_e and (%) removal was evaluated using the following equations:

$$q_e = \frac{(C_o - C_e)\,V}{W} \quad (1)$$

$$\%\,Removal = \frac{(C_o - C_e)}{C_o} \quad X\,100 \quad (2)$$

Where; C_O is the initial ion concentration in mg/l, Ce is the metal ion concentration at equilibrium in mg/l, V is the volume of metal ion solution in litres, and W is the weight of adsorbent used in gram.

2.6 Adsorption kinetics

Kinetic models are time dependent models that can be used to examine the rate of adsorption process and the potential rate-controlling step on the adsorbent surface [24, 2]. In order to analyze the adsorption kinetics of lead (II) ions, the pseudo-first order, pseudo-second order, Elovich equation and intra-particle diffusion, were applied to the experimental data. A simple kinetic form of the equations are given as:

2.6.1 *Pseudo-first-order:* The pseudo first order kinetic model [25], was given by the linear equation

$$\log(q_e - q_t) = \log q_e - \frac{K_1}{2.303}(t) \quad (3)$$

Where q_e and q_t are the amount of metal ion adsorbed (mg/g) at equilibrium and time, t, respectively. K_1 is the first-order reaction rate constant (min^{-1}). A plot of log (q_e-q_t) versus t, gives a linear relationship, from which the value of K_1 and q_e can be determine from the slope and intercept [26].

2.6.2 *Pseudo-second-order:* The linear form of the pseudo second order kinetic rate is given as [27]:

$$\frac{t}{q_t} = \frac{1}{K_2 q_e^2} + \frac{t}{q_e} \qquad (4)$$

Where q_e is the amount of adsorbate adsorbed per unit mass of adsorbent at equilibrium (mg/g), q_t is the amount of adsorbate adsorbed at contact time t (mg/g) and K_2 is the pseudo-second-order rate constant ($gmg^{-1}min^{-1}$). A plot of t/q_t versus t gives a linear relationship, from which q_e and K_2 can be determined from the slope and intercept [28].

2.6.3 *Elovich model:* This model describes the kinetics of chemisorptions. It was first developed to described the chemisorptions of gas into solids [29], and also valid for heterogenous surface systems. The linear form of the equation is expressed as:

$$q_t = \frac{1}{\beta}\ln(\alpha\beta) + \frac{1}{\beta}\ln(t) \qquad (5)$$

Qt denotes the quantity of lead (II) ions adsorbed (mg/g) at any given time. Where α (min/mg/g) and β (g/mg) are the Elovich constants obtained from the slope and intercept of the linear plot of q_t versus ln (t).

2.6.4 *The intraparticle diffusion model:* This model is based on the theory reported by researchers [30], to identify the diffusion mechanism and rate controlling steps affecting the kinetics of adsorption [31]. According to this theory, the adsorbate uptake qt varies almost proportionally with the square root of the contact time, $t^{1/2}$ rather than t, as shown in Eq.(6).

$$q_t = K_{id}.(t)^{\frac{1}{2}} + I \qquad (6)$$

Where I (mg/g), is the constant which is proportional to the boundary layer thickness and K_{id} ($mg/g\ min^{-1/2}$) is the intraparticle diffusion rate constant. Both can be obtained from the intercept and slope of the plot of q_t versus $t^{1/2}$

2.7 Thermodynamic study of adsorption

Thermodynamic parameters like adsorption heat and enthalpy change play an important role in predicting adsorption behavior and they are strongly dependent on temperature [32]. Thermodynamic parameters evaluated for lead (II) ion adsorption onto MCSAC are the Free energy change (ΔG), Enthalpy change (ΔH) and Entropy change (ΔS). These parameters were calculated using the following equation [33].

$$\Delta G = -RT\ln ke \qquad (7)$$

Where ke = q_e/Ce; ke is the thermodynamic equilibrium constant (l/g); q_e is the amount or concentration of lead ion adsorbed per unit mass of the adsorbent (mg/g); Ce is the equilibrium concentration of Pb^{2+} in solution (mg/l); R is the universal gas constant (8.314 $Jmol^{-1}K^{-1}$); T is the temperature in Kelvin (K). Also, from the first law of thermodynamic;

$$\Delta G = \Delta H - T\Delta S \qquad (8)$$

Substituting equation (7) into equation (8), and re-arranging the them gives;

$$\ln ke = -\Delta H/RT + \Delta S/R \qquad (9)$$

The values of ΔH and ΔS were determined from the slope and intercept of the plot of lnke versus 1/T. That is, Slope = ΔH/R and intercept = ΔS/R. Gibb's free energy change of sorption (ΔG) was calculated using equation (13).

2.8 Statistical analysis

Data was analyzed using Microsoft Excel 2007.

3. Results and Discussion

3.1 Characterization of activated carbon

3.1.1 Fourier Transform Infrared Spectroscopy (FTIR)

Functional groups of adsorbents not only affect the adsorption behaviour, but also dominate the adsorption mechanism [34]. From Figure 1.0, FTIR of the MCSAC showed a strong, broad absorption band at 3879.178 and 3231.759 cm^{-1} due to the O-H stretching and inter-molecular bending frequency. The C-H stretching vibration at 3031.678 – 2970.288 cm^{-1} indicates the presence of alkane (sp3) stretching vibration functional group. The stretch vibrations of C=O in ketones and aldehydes in the range of 1869.205-1702.776 cm^{-1}, which may be attributed to aliphatic ketones, aldehydes and carboxylic esters that formed. The peak found at 2178.303-2089.274 cm^{-1} corresponds to the C≡N stretching vibration of the cyanates of nitrile groups. The C=C stretching vibrations at 1609.396 cm^{-1} is assigned to alkenes and aromatic stretching vibration functional groups. The C-O-C and C-O groups at 1133.473-931.543 cm^{-1} indicates the stretching vibrations of carbohydrates. The The peak at 727.0389 cm^{-1} in the adsorbent corresponds to the strong C-H and C-Cl bend of the aromatic bonds alkenes and halogeno compounds.

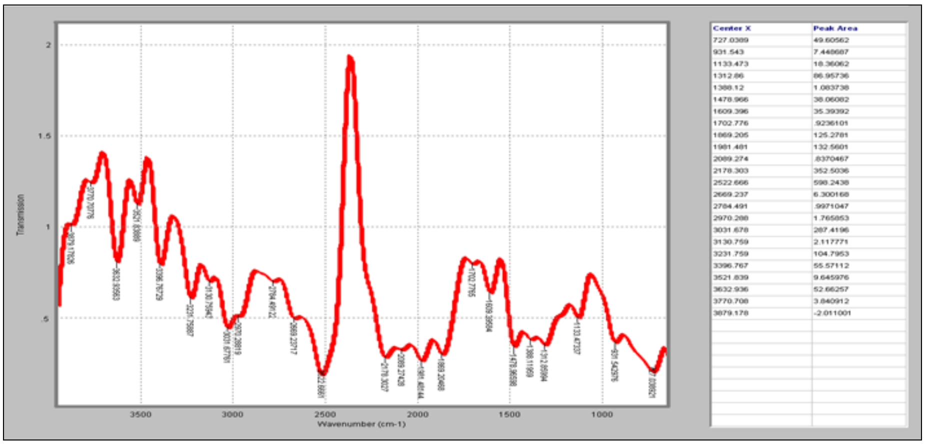

Center X	Peak Area
727.0389	49.60562
931.543	7.448687
1133.473	18.36062
1312.86	86.95736
1388.12	1.083738
1478.966	38.06082
1609.396	35.39392
1702.776	.9236101
1869.205	125.2781
1981.481	132.5601
2089.274	.8370467
2178.303	352.5036
2522.666	598.2438
2669.237	6.300168
2784.491	.9971047
2970.288	1.765853
3031.678	287.4196
3130.759	2.117771
3231.759	104.7953
3396.767	55.57112
3521.839	9.645976
3632.936	52.66257
3770.708	3.840912
3879.178	-2.011001

Fig 1: FTIR spectrum of MCSAC

3.1.2 Energy Dispersive X-ray Spectroscopy (EDX) Analysis

The elemental composition of the adsorbent (MCSAC) was determined based on the fundamental principle that a unique atomic structure allowing unique set of peaks on it X-ray emission [35]. From the Table 1.0 shown below, the major elements present in MCSAC are C, Ta and O while the minor elements are N, Na, F, Si, Cl, P, S, and Al. Also, it is observed that Carbon (C) is the dominant with atomic and weight concentrations of 95.75 and 87.17 respectively.

Table 1: Elemental composition of adsorbent

Elemental composition (%)					
Adsorbent	**Element Number**	**Element Symbol**	**Element Name**	**Atomic Conc.**	**Weight Conc.**
MCSAC	6	C	Carbon	95.75	87.17
	73	Ta	Tantalum	0.60	8.26
	8	O	Oxygen	2.53	3.07
	7	N	Nitrogen	0.76	0.81
	11	Na	Sodium	0.10	0.17
	9	F	Fluorine	0.09	0.13
	14	Si	Silicon	0.04	0.09
	17	Cl	Chlorine	0.03	0.09
	15	P	Phosphorus	0.04	0.09
	16	S	Sulfur	0.03	0.08
	13	Al	Aluminium	0.02	0.05

3.2 Adsorption kinetics

To further study the mechanism of adsorption process, the earlier mentioned kinetic models were applied simultaneously. The results are listed in Table 2.0. Negative differences (values) of equilibrium adsorption capacity (q_e-q_t) between the experiment and calculation was observed, indicating a poor pseudo first-order fit to the experimental data. And examination of the data shows that the pseudo-first-order kinetic model is not applicable to Pb (II) adsorption onto MCSAC at both different temperatures (293K and 313K). However, the adsorption rate constants (k_1 and k_2) of pseudo-second order at different temperatures of 20 °C and 40 °C respectively in Table 2.0 shows that its rate constants of adsorption decreases with the increasing temperature, which reveals that this adsorption may be controlled by physical adsorption. Pseudo-second order show greater correlation coefficient (R^2=1) at 20 °C and (R^2=0.9981) at 40 °C than that of other models. This shows the applicability of the second-order kinetic model over other models as seen in Table 2.0 and Figure 2.0.

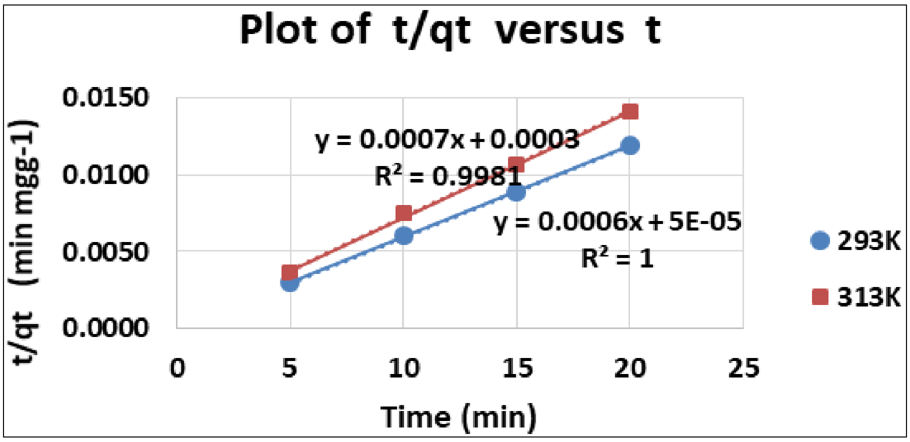

Fig 2: Pseudo-Second-Order kinetic plots for the adsorption of Pb (II) at 20 °C (293K) and 40 °C (313K) onto MCSAC

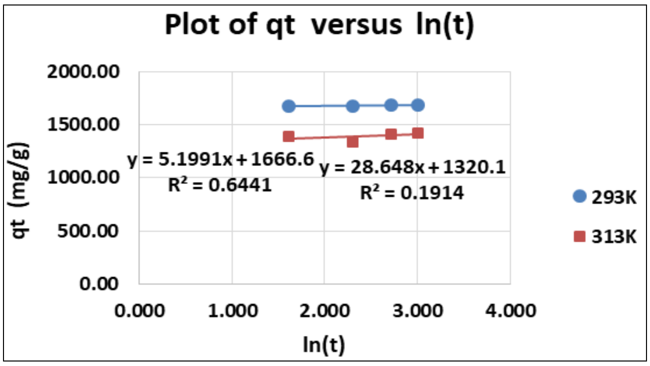

Fig 3: Elovich model plots for the adsorption of Pb (II) at 20 °C (293K) and 40 °C (313K) onto MCSAC

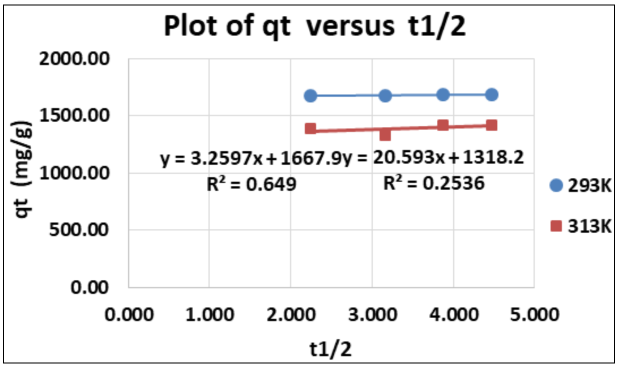

Fig 4: Intraparticle diffusion plots for the adsorption of Pb (II) at 20 °C (293K) and 40 °C (313K) onto MCSAC

Table 2: Kinetic adsorption parameters for Pb (II) ions onto MCSAC adsorbents

Temperature	**Pseudo-first order kinetic model constants**			
(K)	k (g/mg. min)	q_e (mg g^{-1})	R^2	Equations
293	0.0072	1666.7	1.0000	$t/q_t = 0.0006t + 5e\text{-}05$
313	0.0016	1428.6	0.9981	$t/q_t = 0.0007t + 0.0003$
Temperature	Elovich model kinetic model constants			
(K)	α (mg/g.min)	β (g/mg)	R^2	Equations
293	3.16e+138	5.1991	0.6441	$q_t = 5.1991\ln(t) + 1666.6$
313	3.59e+18	28.648	0.1914	$q_t = 28.648\ln(t) + 1320.1$
Temperature	Intraparticle diffusion kinetic model constants			
(K)	K_{id} (mg/g $min^{1/2}$)	I	R^2	Equations
293	3.2597	1667.9	0.649	$q_t = 3.2597t^{1/2} + 1667.9$
313	20.593	1318.2	0.2536	$q_t = 20.593t^{1/2} + 1318.2$

3.3 Thermodynamic study

The effect of temperature was investigated in the temperature range 20 °C to 80 °C, and from Table 3.0, the amount of Pb (II) ions adsorbed (q_e) decreased from 1687.75 mg/g to 1656.10 mg/g as the temperature increased from 293K to 353K, indicating that the uptake of Pb (II) ions onto MCSAC adsorbent decreased as the operating temperature increases. Figure 5.0 shows Van't Hoff plot [36], from which ΔH° and ΔS° in equation (9) were obtained using the values of the equilibrium constants obtained at various temperatures as shown in Table 3.0. The negative value of ΔG° at elevated temperature indicates the spontaneity of the process, and shows that the adsorption is highly favorable for Pb^{2+} ions and progresses more favorably at higher temperature due to a greater driving force of adsorption [37]. The more the negative value of ΔG° the higher the adsorption driving force and the increase of these values with the increase of temperature indicates a lower adsorption at higher temperature [36]. The negative values of ΔH° indicated that adsorption process was exothermic. Similarly, the negative value obtained for ΔS° shows the decrease disorder and randomness at the MCSAC/solution interface during the adsorption process [36, 24].

Table 3: Thermodynamic Parameters of Pb (II) ions adsorption by MCSAC

Temp (K)	**(1/K)**	**Ce**	**q_e (mg/g)**	**ke (Lg^{-1})**	**ln ke**	**ΔG° (KJ mol^{-1})**	**ΔH° (KJ mol^{-1})**	**ΔS° (J $mol^{-1}K^{-1}$)**
293	0.0034	0.167	1687.75	10106.287	9.2209	-22.462	-25.144	-8.137
313	0.0032	0.211	1685.55	7988.389	8.9857	-23.383		
333	0.0030	0.632	1664.50	2633.703	7.8761	-21.806		
353	0.0028	0.800	1656.10	2070.125	7.6354	-22.409		

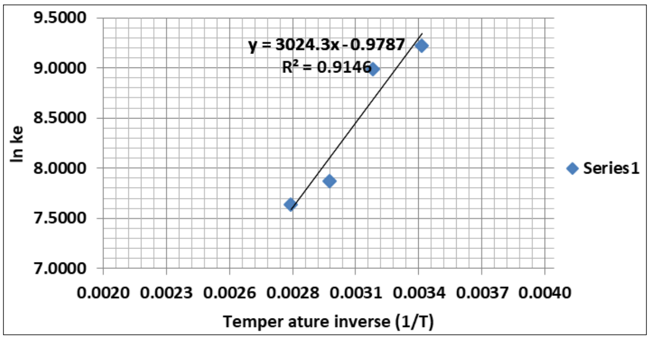

Fig 5: Plot of ln ke versus 1/T for the adsorption of Pb (II) ions onto MCSAC

3.4 Activation energy (Ea)

This is the minimum amount of energy which the reactant molecules must possess to initiate a chemical adsorption [38]. This can be determined from the Arrhenius equation expressed in linear form as given below:

$$\ln k = -\frac{Ea}{RT} + \ln A \qquad (10)$$

where A (g/mg min) is the Arrhenius constant, it is also known as frequency factor; Ea (J/mol) is the activation energy; k is the pseudo-second order rate constant, T (K) is the temperature of the solution; and R (8.314 J/mol K) is the ideal gas constant.

At various temperatures, activation Energy can be determined from the slope of the straight line of plotting lnk versus 1/T. Activation energy can also be calculated directly given two known temperatures and a rate constant at each temperature. We can write equation (12) at two given temperatures T_1 and T_2 as well as the rate constant ks_1 and ks_2 [39, 40]:

$$\ln ks_1 = -\frac{Ea}{RT_1} + \ln A \qquad (11)$$

$$\ln ks_2 = -\frac{Ea}{RT_2} + \ln A \qquad (12)$$

Substracting equation (12) from (11) gives;

$$\ln \frac{ks_1}{ks_2} = \frac{Ea}{R}\left(\frac{1}{T_2} - \frac{1}{T_1}\right) \qquad (13)$$

Where, ks_1 and ks2 represent the pseudo-second order rate constant at 20 °C (T_1) and pseudo-second order rate constant at 40 °C (T_2) respectively.

The above equations expresses the dependence of adsorption rate constant on temperature. From Table 4.4, the adsorption rate constants decrease from 0.0072 to 0.0016 g/gm.min with increasing temperature from 20 °C to 40 °C. And according to [41], if the Ea value is less than 40 $kJmol^{-1}$ the activation energy will be low, the reaction will be faster and physical adsorption, but when the Ea value is ranged from 50-800 $kJmol^{-1}$, the activation energy is higher and slower in chemical adsorption [42].

For the Pb (II) ions adsorption on MCSAC in this study, the apparent activation energy of the pseudo-second order kinetic model is obtained to be -57.341 kJ mol^{-1}. And the apparent rate constant (k) decreased with increasing temperature as seen in Table 3.0. However, the activation energy (Ea) is less than 40 kJ mol^{-1} which shows that this adsorption process is slow and exothermic. The negative activation energy also indicates that energy barriers are absent in the adsorption process, and when temperature is raised the colliding molecules are separated quickly far apart from capturing one another [43, 40]. Also, according to report by [44], sorption processes exhibiting negative activation energies are exothermic and proceeds at lower temperatures. As the temperature is increased, the adsorbate species solubility increases, and consequently causing the force of interaction between the adsorbate and solvent stronger than those between adsorbate and adsorbent. As a result, the adsorbate is more difficult to adsorb [44]. Hence, the low value of the activation energy (*Ea* << 40 kJ/mol) indicated that the adsorption process of lead (II) ions onto MCSAC is physical adsorption and rate-limiting step [41].

Table 4: Activation energy for adsorption of heavy metal ions and other adsorbate molecules onto various low cost adsorbents

Adsorbent	Adsorbate	Ea (kJmol-1)	Reference
Laterite nickel ores	Pb (II)	7.6	[45]
Peanut shell	Pb(II)	42.4	[46]
Albizia lebbeck pods	Pb(II)	33.161	[47]
Alluvia soil	Pb(II)	-38.33	[57]
Polymer-modified coconut shell	Pb(II)	-57.341	This study
Cation exchanger derived from tamarind fruit shell	Cu (II)	10.84	[48]
Peanut shell	Cu (II)	17.02	[49]
Aluminum oxide nanopowder	Fe (III)	25.29	[50]
Wineyard pruning waste	Cr(III)	-15.65	[51]
Walnut hull	Cr (VI)	102.78	[52]
Chitosan intercalated montmorillonite	Methyl orange	-16.35	[53]
Resin D301	Glyphosate	83.11	[54]
Eggshell Powder	Brilliant Green Dye	-15.88	[55]

4. Conclusion

Investigation of the potential effect of the improved coconut shell activated carbon (MCSAC) was studied. The FTIR showed some functional groups such as hydroxyl, carboxylic, carbonyl, nitrile, aliphatic and aromatic compounds that was added to improve the adsorbent physical properties [56]. The EDX analysis showed that Carbon (C) is the dominant element of the adsorbent with atomic and weight concentrations of 95.75 and 87.17 respectively as shown in Table 4.0. The equilibrium results obtained agreed with the findings that the effectiveness of Pb (II) ion adsorption under optimized conditions (concentration 200 mg/l, contact time 15 min, dosage 0.2 g/10ml, temperature 20 ^oC, pH 8) strongly dependent on the quality improvement of the adsorbents. Also, from Table 12.0, the amount of Pb (II) ions adsorbed (q_e) decreased from 1687.75 mg/g to 1656.10 mg/g as the temperature increased from 293K to 353K, indicating that the uptake of Pb (II) ions onto MCSAC adsorbent decreased as the operating temperature increases. Thus, The results support that an improved coconut shell activated with inorganic polymer has the potential to be developed into an effective adsorbent for the removal of lead from effluent and contaminated water. The experimental data indicate that the process follows pseudo-second-order kinetics model. The thermodynamic data indicate that the processes is spontaneous, slow and exothermic over range of temperature. The values of enthalpy (ΔH), Gibb's free energy (ΔG), entropy (ΔS) and activation energy (Ea) indicate that the adsorption process is physical sorption.

5. References

1. Duruibe JO, Ogwuegbu MOC, Egwurugwu JN. Heavy metal pollution and human biotoxic effects. International Journal of Physical Sciences. 2007; 2(5):112-118.
2. Ogbeide OM, Ezeh EC, Okpara OG. Isotherms, kinetics and equilibrium Studies of adsorption of Lead (II) ions from aqueous solutions Using Polymer-Modified Coconut Shell Activated Carbon (MCSAC). IOSR Journal of Environmental Science, Toxicology and Food Technology (IOSR-JESTFT). 2019; 13(8):28-43.
3. WHO. Lead Poisoning and Health. World Health Organization, 2018. (https://www.who.int/news-room/fact-sheets/detail/lead-poisoning-and-health).
4. Caffo M, Caruso G, La Fata G, Barresi V, Visalli M, Venza M, *et al*. Heavy Metals and Epigenetic Alterations in Brain Tumors. Current Genomics, 2014; 15:457-463.
5. Masindi V, Muedi KL. Environmental Contamination by Heavy Metals. Intechopen, 2018, 115-133.
6. Samiey B, Cheng CH, Wu J. Organic-Inorganic Hybrid Polymers as Adsorbents for Removal of Heavy Metal Ions from Solutions: A Review. Materials, 2014; 7:673-726.
7. Mandina S, Chigondo F, Shumba M, Nyamunda BC, Sebata E. Removal of chromium (VI) from aqueous solution using chemically modified orange (citrus cinensis) peel. IOSR Journal of Applied Chemistry. 2013; 6(2):66-75.
8. Kismir Y, Aroguz AZ. Adsorption characteristics of the hazardous dye brilliant green on Saklikent mud. Chem. Eng. J, 2011; 172:199-206.
9. Ghaedi M, Sadeghian B, Pebdani AA, Sahraei R, Daneshfar A, Duran C, *et al*. Kinetics, thermodynamics and equilibrium evaluation of direct yellow 12 removal by adsorption onto silver nanoparticles loaded activated carbon. Chem. Eng. J, 2012; 187:133-141
10. Iqbal MJ, Ashiq MN. Adsorption of dyes from aqueous solutions on activated charcoal. J Hazard. Mater, 2007; 139:57-66.
11. Onundi YB, Mamun AA, Al Khatib MF, Ahmed YM. Adsorption of copper, nickel and lead ions from synthetic semiconductor industrial wastewater by palm shell activated carbon. Int. J Environ. Sci. Tech. 2010; 7(4):751-758.
12. Abdulkarim M, Abu Al-Rub F. Adsorption of Lead Ions from Aqueous Solution onto Activated Carbon and Chemically-modified Activated Carbon Prepared from Date Pits. Adsorption Science and Technology. 2003; 22(2):119-134.
13. Nwosu FO, Olu-Owolabi BI, Adebowale KO. Kinetics and Thermodynamic Adsorption of Pb (II) and Cd (II) Ions from Used Oil onto Thevetia Neriifolia Nutshell Active Carbon. Current Research in Chemistry. 2012; 4(2):26-40.
14. Thajeel, A.S. Isotherm, Kinetic and Thermodynamic of Adsorption of Heavy Metal Ions onto Local Activated Carbon. Aquatic Science and Technology. 2013; 1(2):52-77.
15. Kumar PS, Vincent C, Kirthika K, Kumar KS. Kinetics And Equilibrium Studies Of Pb^{2+} Ion Removal From Aqueous Solutions By Use Of Nano-Silversol-Coated Activated Carbon. Brazilian Journal of Chemical Engineering. 2010; 27(2):339-346.
16. Haghdoost G, Aghaie H, Monajjemi M. Investigation of Langmuir and freundlich adsorption isotherm of Pb^{2+} ions by micro powder of cedar leaf. Journal of Physical

and Theoretical Chemistry. 2016; 13(3):289-296.

17. Aderibigbe AD, Ogunlalu OU, Oluwasina OO, Amoo IA. Adsorption studies of Pb^{2+} from aqueous solutions using unmodified and citric acid-modified plantain (musa paradisiacal) peels. IOSR journal of applied chemistry. 2017; 10(2):30-39.
18. Hajji S, Mzoughi N. Kinetic, equilibrium and thermodynamic studies for the removal of lead ions from aqueous solutions by using low cost adsorbents: a comparative study. IOSR Journal of Applied Chemistry. 2018; 11(7):12-24.
19. Jahangard A, Sohrabi M, Beigmohammadi Z. Sorption of Lead (II) Ions on Activated Coconut Husk. Iranian Journal of Toxicology. 2016; 10(6):23-29.
20. Jyotsna G, Kadirvelu K, Rajagopal C, Garg VK. Removal of lead (II) by adsorption using treated granular activated carbon: Batch and column studies. Journal of Hazardous Materials B125, 2005, 211-220.
21. Song C, Wu S, Cheng M, Tao P, Shao M, Gao G, *et al*. Adsorption Studies of Coconut Shell Carbons Prepared by KOH Activation for Removal of Lead(II) From Aqueous Solutions. Sustainability, 2013; 6:86-98.
22. Sener S, Erdemoglu M, Asilturk M, Sayilkan H. The Effect of Silane Modification on the Adsorptive Properties of Natural Pyrophylite and Synthetic Titanium-Based Powders Prepared by the Sol-Gel Process. Turk. J Chem, 2005; 29:487-495.
23. Ezeh EC, Ukoha PO, Bulus H, Nweze BN, Nwagu NI, Nsude PO, *et al*. Adsorption isotherms and kinetic studies of Pb2+ and Cu2+ sorption by semicarbazide immobilized polysiloxane as material for water purification. A publication of Chemical Society of Nigeria, Anachem Journal. 2019; 9(1):1652-1664.
24. Kocer NN, Uslu G, Cuci Y. The adsorption of Zn (II) ions onto chitin: determination of equilibrium, kinetic and thermodynamic parameters. Adsorption Science and Technology. 2008; 26(5):333-344.
25. Lagergren S. About the theory of so-called adsorption of soluble substances. K. Sven. Vetenskapsakad. Handlingar Band, 1898; 24:1-39.
26. Pathania D, Sharma S, Singh P. Removal of methylene blue by adsorption onto activated carbon developed from Ficuscaricabast. Arabian Journal of Chemistry, 2017; 10:1445-1451.
27. Ho YS, Mckay G, Wase DAJ, Forster CF. Study Of The Sorption Of Divalent Metal Ions On To Peat. Adsorption Science and Technology. 2000; 18(7):639-650.
28. Bhattacharyya KG, Sharma A. Kinetics and thermodynamics of methylene blue sorption on neem (Azadirachtaindica) leaf powder. Dyes and Pigments, 2005; 65:51-59.
29. Kumara PS, Ramalingamb S, Kiruphac SD, Murugesanc A, Vidhyadevic T, *et al*. Adsorption behavior of nickel (II) onto cashew nut shell: Equilibrium, thermodynamics, kinetics, mechanism and process design. Chem. Eng. J, 2011; 167:122-131.
30. Weber WJ, Morris JC. Kinetics of adsorption on carbon from solutions. J Sanit. Eng. Div, 1963; 89:31-60.
31. Aljeboree AM, Alshirifi AN, Alkaim AF. Kinetics and equilibrium study for the adsorption of textile dyes on coconut shell activated carbon. Arabian Journal of Chemistry, 2014; 10:S3381-S3393.
32. Rehman R, Abbas A, Murtaza S, Anwar J, Mahmud T, Akbar S, *et al*. Adsorption parameters optimization for removal of alizarin red-S and brilliant blue FCF dyes from water using Abelmoschus esculentus stem powder. Journal of Chemical Society of Pakistan. 2013; 35(2):443-448.
33. Hameed BH, Ahmad AA, Aziz N. Isotherm, Kinetics and Thermodynamics of Acid Dye Adsorption on Activated Palm Ash. Chemical Engineering Journal. 2007; 133(1-3):195-203.
34. Zheng Y, Zhu Y, Wang A. Kapok fiber structure-oriented polyallylthiourea: Efficient adsorptive reduction for Au (III) for catalytic application. Polymer. 2014; 55(20):5211-5217. https://doi.org/10.1016/j.polymer.2014.08.040
35. Goldstein JI, Newbury DE, Joy DC, Lyman CE, Echlin P, Lifshin E, Sawyer L, *et al*. Scanning Electron Microscopy and X-ray microanalysis. Extra Materials http://extras.springer.com. (3rd edition), ISBN 978-1-4613-4615-0215-9, ISBN 978-1-4615-0215-9 (ebook). DOI 10.1007/978-1-4615-0215-9.
36. Piccin JS, Dotto GL, Pinto LAA. Adsorption isotherms and thermochemical data of FD&C red N^{O} 40 binding by chitosan.Brazilian Journal of Chemical Engineering. 2011; 28(2):295-304.
37. Meroufel B, Benali O, Benyahia M, Benmoussa Y, Zenasni MA, *et al*. Adsorptive removal of anionic dye from aqueous solutions by Algerian kaolin: characteristics, isotherm, kinetic and thermodynamic studies. Journal of Material and Environmental Source. 2013; 4(3):482-491.
38. Baily SE, Olin TJ, Bricka RM, Adrian DD. A review of potentially low-cost adsorbents for heavy metals. Water Research. 1999; 33(11):2469-2479.
39. Ibemesi JA. Physical Chemistry for Tertiary Institutions, Part 1(second edition). Department of pure and industrial chemistry, university of Nigeria nsukka, 2004. ISBN 978-35255 8-1. Pg 1-375
40. Atkins P, de Paula J. Elements of Physical Chemistry, (Fifth edition). New York. Oxford University Press, 2009, Pp 232-252.
41. Morais LC, Freitas OM, Goncalves EP. Vasconcelos, L.T. and Beca, C.G.G. Relative Dyes Removal from wastewaters by Adsorption on Eucalyptus bark: Variable that define the process. Water Res, 1999; 33:979-988.
42. Zhou Wei, Tang Yu, Xie Huan, Liu Cha, Yang Dajian, Chen Xinzi, *et al*. Kinetics and thermodynamics of absorption of ganciclovir by ion exchange resin. J. Chin. Pharm, 2009; 17:1327-1331.
43. Kobiraj R, Gupta N, Kushwaha AK, Chattopadhyaya MC. Determination of equilibrium, kinetic and thermodynamic parameters for the adsorption of Brilliant Green dye from aqueous solutions onto eggshell powder. Indian Journal of Chemical Technology, 2012; 19:26-31.
44. Saha P, Chowdhury S. Insight into Adsorption Thermodynamics, Thermodynamics, Prof. Mizutani Tadashi (Ed.), ISBN: 978-953-307-544-0, InTech, 2011. Available from: http://www.intechopen.com/books/thermodynamics/insight-into-adsorption-thermodynamics
45. Mohapatra M, Khatun S, Anand S. Kinetics and thermodynamics of lead (II) adsorption on lateritic nickel ores of Indian origin. Chemical Engineering

Journal. 2009; 155(1-2):184-190. https://doi.org/10.1016/j.cej.2009.07.035

46. Taşar S, Özer A. A Thermodynamic and Kinetic Evaluation of the Adsorption of Pb (II) Ions Using Peanut (*Arachis Hypogaea*) Shell-Based Biochar from Aqueous Media. Pol. J Environ. Stud. 2019; 29(1):293-305.
47. Mustapha S, Shuaib DT, Ndamitso MM, Etsuyankpa MB, Sumaila A, Mohammed UM, *et al*. Adsorption isotherm, kinetic and thermodynamic studies for the removal of Pb(II), Cd(II), Zn(II) and Cu(II) ions from aqueous solutions using *Albizia lebbeck* pods. Applied Water Science, 2019; 9:142.
48. Anirudhan TS, Radhakrishnan PG. Thermodynamics and kinetics of adsorption of Cu (II) from aqueous solutions onto a new cation exchanger derived from tamarind fruit shell. Journal of Chemical Thermodynamics. 2008; 40(4):702-709. ISSN: 0021-9614.
49. Zhu CS, Wang LP, Chen WB. Removal of Cu (II) from aqueous solution by agricultural by product: Peanut hull. Journal of Hazardous Materials. 2009; 168(2-3):739-746. ISSN: 0304-3894.
50. Mahmoud MA. Kinetics and thermodynamics of Aluminum Oxide Nanopowder as Adsorbent for Fe (III) from Aqueous Solution. Beni-Suef University Journal of Basic and Applied Sciences, 2015; 4:142-149.
51. Karaoglu MH, Zor S, Ugurlu M. Biosorption of Cr (III) from solutions using vineyard pruning waste. Chemical Engineering Journal, 2010; 159:98-106. ISSN:1385-8947.
52. Wang XS, Li ZZ, Tao SR. Removal of chromium (VI) from aqueous solution using walnut hull. Journal of Environmental Management. 2009; 90(2):721-729. ISSN: 0301-4797.
53. Umpuch C, Sakaew S. Removal of methyl orange from aqueous solutions by adsorption using chitosan intercalated montmorillonite. *Songklanakarin.* J. Sci. Technol. 2013; 35(4):451-459.
54. Chen FX, Zhou CR, Li GP, Peng FF. Thermodynamics and kinetics of glyphosate adsorption on resin D301. Arabian Journal of Chemistry, 2012; 9:S1665-S1669
55. Kobiraj R, Gupta N, Kushwaha AK, Chattopadhyaya MC. Determination of Equilibrium, Kinetic and Thermodynamic Parameters for the Adsorption of Brilliant Green Dye from Aqueous Solutions onto Eggshell Powder. Indian Journal of Chemical Technology, 2011; 19:26-31.
56. Anierobi PO. Modification of Coconut shell Activated Carbon with an azo ligand for the removal of Cd^{2+}, Pb^{2+} and Ni^{2+} from polluted water. A Masters project submitted to the department of Industrial Chemistry, Faculty of Physical Sciences, University of Nigeria, Nsukka, 2014.
57. Das B, Mondal NK, Bhaumik R, Roy P. Insight into adsorption equilibrium, kinetics and thermodynamics of lead onto alluvial soil. International Journal of Environmental Science and Technology. 2013; 11(4):1101-1114.